Turkish Journal of Electromechanics and Energy
ISSN: 2547-975X
Vol:9, No:1, Page 25-32 (2024)
https://www.scienceliterature.com

AC motor selection in machine design applications

M. E. Kütük[1,*], S. Kapucu[1]

[1] *Department of Mechanical Engineering, Gaziantep University, Gaziantep, Türkiye*

ARTICLE INFO

***Article Type*:**
Selected Research Article [c]

Article History:
Received: 18 December 2023
Revised: 8 March 2024
Accepted: 14 March 2024
Published: 17 April 2024

Editor of the Article:
M. E. Şahin

Keywords:
AC motor selection
Torque-speed curve
Kloss formula
Scotch Yoke mechanism

ABSTRACT

Asynchronous or induction alternating current (AC) motors are frequently used in industry to drive machines. An important feature of most AC motors is the torque-speed curve. The main purpose of this study is to provide a guide on how to create an electromechanical model for a real system and how the selected motor will affect the kinematic and kinetic performances. In this study, it is explained how to define the speed-torque characteristic and obtain an approximate speed-torque graph using the standard catalogue of motor manufacturers and Kloss formulas. Three approaches based on Kloss formulas from literature are introduced and one of them is selected to be used. A Scotch Yoke mechanism used for packaging purposes is chosen as an industrial application. The equation of motion of that mechanism is obtained and a numerical solution is shown. The electromechanical system equation includes the mechanism dynamic model and the Kloss equations containing the catalogue data of the selected motor. At the end of the numerical simulation, the dynamic performance of the system is being evaluated. It is investigated that the selected motor is enough to drive the mechanism. Additionally, the effect of adding a flywheel to the system on the fluctuation of speed is also examined.

Cite this article: M. E. Kütük, S. Kapucu, "AC motor selection in machine design applications," *Turkish Journal of Electromechanics & Energy*, 9(1), pp.25-32, 2024.

1. INTRODUCTION

Electric motors are one of the most commonly used actuator types. They come in a wide variety, including direct current (DC) motors, stepper motors, servo motors, and asynchronous alternating current (AC) motors. Among these, asynchronous or induction alternating current (AC) motors are frequently used in industry to drive machines. An important feature of most induction motors is the torque-speed curve [1, 2].

It is a fact that the selection of a motor for an application is influenced by several factors such as power, speed, torque, physical size, efficiency, duty cycle, ambient temperature and feedback control, braking, desired result, operating environment, and specific application parameters [3]. Although the types of induction motors vary depending on the application area, they are *A* and *B*-type motors given in Figure 1, which are the motor types frequently used in the machinery manufacturing industry. The different torque capacities of standard induction motors are labelled as *A*, *B*, *C* and D in the National Electrical Manufacturers Association (NEMA) [4]. *A*-*B* motor designs are renowned for their high efficiencies and minimal slip, making them suitable for variable/constant torque applications. Design *C* motors were initially crafted to meet the high starting torque demands. However, they have the expense of higher motor losses and reduced efficiency compared to design *B* motors. They can be preferred in pumps and compressors. Meanwhile, Design *D* motors find their niche in applications requiring substantial starting torque or managing high inertia loads, featuring notable characteristics such as high slip and comparatively lower efficiencies. They can be used in applications of impact loads. Important torque values (e.g. starting, pull-up, breakdown, and rated) on the torque–speed curve are shown in Figure 1. The motor is chosen by providing that the system will drive the mechanism or mechanisms and will operate in the "stable region" after the first working zone. The graph showing the starting (start-up) zone -stable zone-stop zones of a motor-driven system created by choosing random values is given in Figure 2. In systems that make frequent stops and starts, these stop-start periods must be short to prevent the motor from overheating. In the system in Figure 2, it is seen that the motor in the stable region fluctuates around its average speed shown by the dotted line, in other words, there is "speed fluctuation". Depending on the application, it may be necessary to add a flywheel to the system to decrease the fluctuation and check whether the motor will provide the necessary torque to drive this flywheel by taking the allowed speed fluctuation coefficient [5, 6].

This paper aims to provide a comprehensive overview of AC motor selection methodologies and considerations in machine design applications. Through a synthesis of academic literature, industry standards, and practical insights, this study will elucidate the key parameters influencing motor selection and propose a

[c] *Initial version of this article was presented at the 5th International Conference of Materials and Engineering Technology (TICMET'23) held on November 13-16, 2023, in Trabzon, Türkiye. It was subjected to a peer-review process before its publication.*

**Corresponding author's e-mail: mekutuk@gantep.edu.tr*

systematic framework for engineers and designers. By addressing the complexities of motor selection, this paper seeks to empower practitioners with the knowledge and tools necessary to make informed decisions and evaluate the performance of their designs.

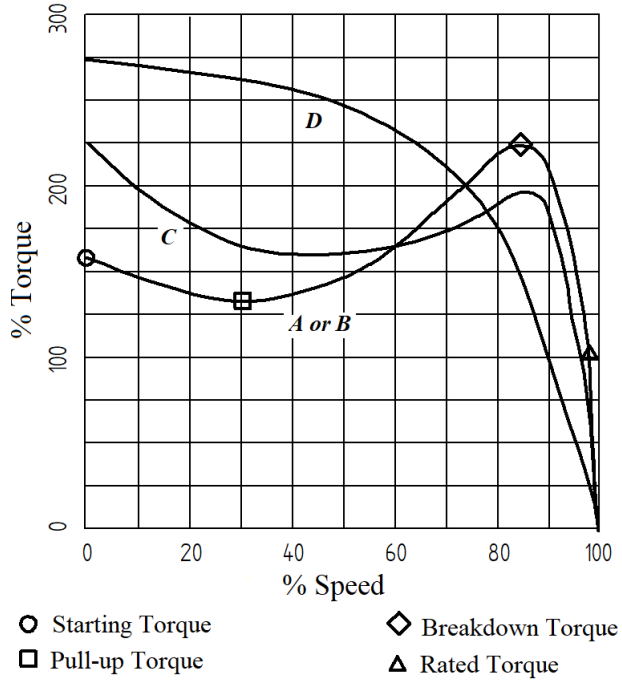

Fig. 1. Typical speed-torque curves for designs A, B, C and D, classified by speed-torque curves [4].

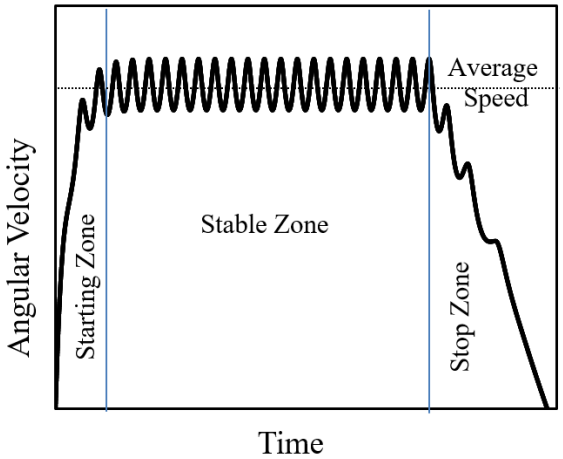

Fig. 2. Working zones of the motor-driven system.

2. DEFINING THE SPEED-TORQUE CHARACTERISTIC FROM MOTOR CATALOG

It is possible to determine the characteristics of the motors from their catalogue data [7, 8]. Kloss formulas can also be used to define the speed-torque characteristic and obtain its graph approximately from the standard catalogue information of motor manufacturers [9, 10]. The synchronous speed of induction motors (N_s) in rev/min; is expressed in terms of alternating current frequency (f) and number of motor poles (p) as follows:

$$N_s = \frac{120\,f}{p} \tag{1}$$

The change in speed of the motor shaft when the motor is loaded is called the slip (S) and is given in Equation (2).

$$S = \frac{N_s - n}{N_s} \tag{2}$$

n is the motor shaft speed. The nominal slip value (S_n) s is expressed in Equation (3) using the nominal (rated) speed (N_n),

$$S_n = \frac{N_s - N_n}{N_s} \tag{3}$$

2.1. Torque-Speed Equation 1 (TSE1)

In the study conducted by Kral *et al.* [11], it is stated that the equation of the torque-speed graph can be found approximately as Equation (4), using data that can be obtained from manufacturer catalogues:

$$M = \frac{2M_{bd}}{\frac{S}{S_{bd}} + \frac{S_{bd}}{S}} \tag{4}$$

$$\text{where } \frac{S_{bd}}{S_n} = \frac{M_{bd}}{M_n} + \sqrt{\left(\frac{M_{bd}}{M_n}\right)^2 - 1} \tag{5}$$

This Kloss equation states the relationship between the breakdown (bd) torque and the breakdown slip value and an arbitrary load point determined by the torque and the slip.

2.2. Torque-Speed Equation 2 (TSE2)

In the study conducted by Buksnaitis [12], the critical slip equation is defined in Equation (6) to determine the torque speed graph with data that can be taken from manufacturer catalogues.

$$S_{cr} = S_n \frac{\frac{M_{bd}}{M_n} + \sqrt{\left(\frac{M_{bd}}{M_n}\right)^2 - 1 + 2S_n\left(\frac{M_{bd}}{M_n} - 1\right)}}{1 - 2S_n\left(\frac{M_{bd}}{M_n} - 1\right)} \tag{6}$$

According to the critical slip value of the rotor, the torque-speed equations are determined as follows:

If $0 < S < S_{cr}$

$$M = \frac{2M_{bd}}{\frac{k_1}{S^\alpha} + \frac{S^\alpha}{k_1}} \tag{7}$$

where

$$\alpha = \log b / \log(S_{cr} / S_n),\ b = \frac{M_{bd}}{M_n} + \sqrt{\left(\frac{M_{bd}}{M_n}\right)^2 - 1},\ k_1 = bS_n^\alpha \tag{8}$$

If $S_{cr} < S < 1$

$$M = \frac{2M_{bd}}{\frac{k_2}{S^{\beta}} + \frac{S^{\beta}}{k_2}} \tag{9}$$

where

$$\beta = \log k_2 / \log S_{cr}\,,\; k_2 = \frac{M_{bd}}{M_{st}} - \sqrt{\left(\frac{M_{bd}}{M_{st}}\right)^2 - 1} \tag{10}$$

2.3 Torque-Speed Equation 3 (TSE3)

In the study conducted by Aree [13], the approximate torque-speed equation is expressed as Equation (11).

$$M = \frac{2\left(1+\varepsilon S_b\right)M_{bd}}{\frac{S_n}{S_b} + 2\varepsilon S_b + \frac{S_b}{S_n}} \tag{11}$$

where $S_b = \dfrac{-b+\sqrt{b^2-4ac}}{2a}$

$$a = S_n - \left(S_n\frac{M_{bd}}{M_{st}} - 1\right)\left(\frac{M_n}{M_{bd}}\right),$$

$$b = -2S_n + 2S_n\left(\frac{M_{bd}}{M_{st}}\right)\left(\frac{M_n}{M_{bd}}\right),$$

$$c = S_n - S_n\left(1+S_n\left(\frac{M_{bd}}{M_{st}} - 1\right)\right)\left(\frac{M_n}{M_{bd}}\right),$$

$$\varepsilon = \frac{1}{2}\frac{\left(1+S_b^2 - 2\left(\frac{M_{bd}}{M_{st}}\right)S_b\right)}{S_b^2\left(\frac{M_{bd}}{M_{st}} - 1\right)} \tag{12}$$

It is possible to show the torque speed characteristics of a randomly selected motor catalogue information by using the above-mentioned approaches. The motor in the seventh row of the catalogue [14] given in Figure 3 can be selected. Afterwards, it is possible to make a comparison. The power of the selected motor is 2.2 kW, the nominal speed (N_n) is 1450 rpm, the nominal torque (M_n) is 14.5 Nm, the ratio of starting torque to nominal torque (M_{st}/M_n) is 2.8, and the ratio of breakdown torque to nominal torque (M_{bd}/M_n) is 3.6. The curves of the torque-speed equations (TSE1, TSE2, and TSE3) are given in Figure 4. Please note that the rated torque at full load speed (n=1450 rpm) is the same in all torque-speed graphs.

As can be seen from the graph of the torque-speed Equation 1 mentioned in section 2.1, it is clear that the starting torque value is quite small compared to the others. The parts of all torque-speed graphs after the breakdown torques are approximately similar to each other. The take-off time will require longer than expected due to the low starting torque. Therefore, one of the torque-speed Equations (2-3) mentioned in sections 2.1 and 2.2 can be used. The torque equation given in section 2.2 will be used in this study.

400V 50Hz 1500 rev/min IE3

Voltage (V)	Type	Nominal Values								Starting Values		Breakdown Moment	Inertia	Mass	Noise
		Power	Speed	Current	Moment	Power Factor	Efficiency % η			Current	Moment				
		kW	d/d	A	Nm	Cos φ	4/4	3/4	1/2	I_A/I_N	M_A/M_N	M_K/M_N	kgm²	kg	dB(A)
230/400	3EL071M4C	0,25	1435	0,67	1,66	0,71	76,0	75,4	71,5	5,4	2,2	3,0	0,00082	6,80	45
	3EL071M4D	0,37	1435	0,97	2,46	0,70	78,5	78,2	75,0	5,5	2,2	3,1	0,00093	7,50	45
	3EL080M4C	0,55	1450	1,34	3,62	0,73	80,8	80,4	77,0	5,9	2,1	3,1	0,00200	10,5	50
	3EL080M4D	0,75	1450	1,77	4,94	0,74	82,5	82,3	80,0	6,2	2,5	3,4	0,00227	11,6	50
	3EL090S4C	1,10	1450	2,46	7,25	0,76	84,5	84,3	82,0	7,0	2,6	3,6	0,00355	16,3	51
	3EL090L4D	1,50	1445	3,30	9,91	0,77	85,3	85,2	83,0	7,2	2,8	3,8	0,00411	18,0	51
	3EL100L4C	2,20	1450	4,65	14,5	0,79	86,7	87,2	86,0	7,2	2,8	3,6	0,00775	24,4	53
	3EL100L4D	3,00	1450	6,26	19,8	0,79	87,7	88,0	87,0	7,2	2,8	3,6	0,00888	26,7	53
400/690	3EL112M4D	4,00	1460	8,05	26,2	0,81	88,6	88,4	87,5	7,4	2,8	3,8	0,01437	33,9	58
	3EL132S4C	5,50	1465	10,9	36,0	0,81	89,6	90,2	90,0	7,0	3,0	3,4	0,03059	53,4	61
	3EL132M4D	7,50	1465	14,4	48,9	0,83	90,4	90,4	89,4	7,9	3,0	3,8	0,03418	59,5	61
	3EL160M4C	11,0	1465	21,0	71,7	0,83	91,5	92,1	91,7	7,6	2,8	3,3	0,07011	89,2	63
	3EL160L4E	15,0	1465	28,7	97,8	0,82	92,1	92,4	91,9	7,8	2,8	3,6	0,08579	97,5	63
	3EG180M4C	18,5	1475	35,0	120	0,82	92,6	93,2	92,9	7,7	3,0	3,3	0,12901	173	64
	3EG180L4D	22,0	1470	41,4	143	0,82	93,0	93,7	93,7	8,0	3,0	3,4	0,14667	187	64
	3EG200L4D	30,0	1475	54,5	194	0,85	93,6	94,1	94,0	8,0	3,0	3,4	0,28413	258	65
	3EG225S4C	37,0	1478	65,7	239	0,87	93,9	94,5	94,5	8,3	3,2	3,3	0,38229	320	66
	3EG225M4D	45,0	1477	80,0	291	0,86	94,2	94,7	94,7	8,6	3,3	3,2	0,44100	352	67
	3EG250M4D	55,0	1482	95,3	354	0,88	94,6	95,1	95,2	8,7	3,3	3,2	0,73000	470	68
	3EG280S4C	75,0	1485	130	482	0,88	95,0	95,3	95,1	7,9	3,0	3,2	1,40000	646	69
	3EG280M4D	90,0	1485	156	579	0,88	95,2	95,7	95,7	7,9	3,1	3,2	1,50000	670	70
	3EG315S4C	110	1488	191	706	0,87	95,4	95,7	95,3	7,5	2,7	3,0	2,40000	850	72
	3EG315M4D	132	1489	229	846	0,87	95,6	95,9	95,5	7,5	2,7	3,0	2,80000	920	73
	3EG315L4E	160	1490	274	1026	0,88	95,8	96,0	95,7	7,6	2,8	3,1	3,30000	1020	73
	3EG315L4F	200	1491	341	1282	0,88	96,0	96,2	95,9	7,6	2,9	3,1	4,40000	1200	73

Fig. 3. A motor catalog from ELK motor [14].

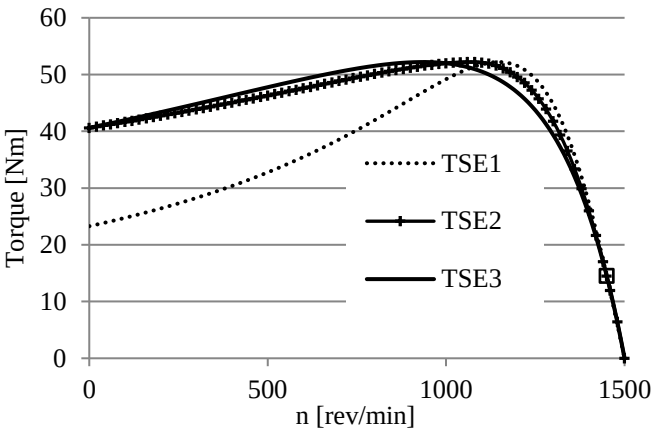

Fig. 4. Curves of torque speed equations.

3. DYNAMIC MODEL OF A SCOTCH-YOKE MECHANISM

The equations of motion for dynamical systems can be stated as the Lagrange equation [15] as depicted in Equation (13).

$$\frac{d}{dt}\left(\frac{\partial L}{\partial \dot{q}_i}\right)-\frac{\partial L}{\partial q_i}=Q_i \qquad i=1,2,...,n \tag{13}$$

where L is the Lagrangian. n is the number of generalized coordinates selected, q is the generalized coordinates, and Q is the generalized force/torque acting on the i^{th} generalized coordinate. It is given in Equation (14).

$$Q_i=\sum_{k=1}^{N}\vec{F}_k\cdot\frac{\partial \vec{r}_k}{\partial q_i} \qquad k=1,2,....,N \tag{14}$$

where r is the coordinate that defines the position of the system forces and/or torques. F is the external force or moment on the axis applied to the application point indicated by r. Generalized forces/moments consist of all forces/moments outside the system. These external forces/moments can be arbitrary functions of generalized coordinates and time. Physically, there can be forces/moments that involve the addition of energy into the system, such as actuation forces/moments, and/or energy dissipation from the system, such as velocity-dependent damping forces/moments of viscous dampers and/or forces/moments that depend on position, velocity, and acceleration due to Coulomb friction.

By definition, the Lagrangian of the system is:

$$L=K-P \tag{15}$$

where K is the total kinetic energy and P is the total potential energy of the system. The Lagrange equation describes the dynamics of the relevant coordinate only. Therefore, for a system with n degrees of freedom, n equations are derived that describe the dynamics of the entire system simultaneously.

The equation of motion of a Scotch Yoke mechanism of a packaging machine is given below. The configuration of the mechanism is shown in Figure 5(a). The centre of mass of the 2nd link, the 3rd link and the 4th link are at A, B and C respectively. It is assumed that the gaps between link 2 and link 3 are negligibly small. The mechanism works in the horizontal plane. F_{14} force acts on link four as a function of θ, as seen in Figure 5(b). It is also assumed that the friction and damping forces are negligibly small. The inertial and dimensional properties of the mechanism; $m_2=2\ kg$, $m_3=4\ kg$, $m_4=6\ kg$, $I_{CG2}=0.02\ kgm^2$, $AB=a_2=350mm$, $AD=x$, $DB=y$, $DH=a_4=450mm$.

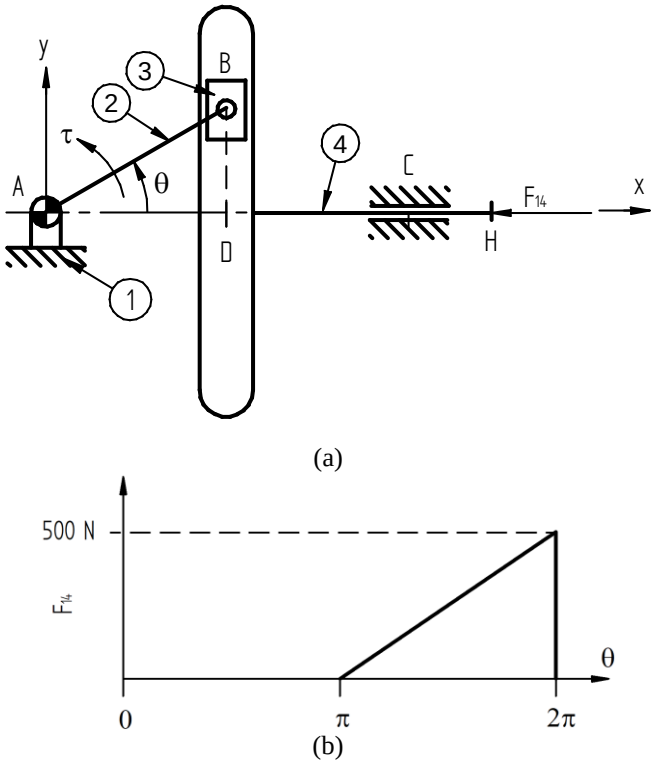

Fig. 5. (a) A Scotch Yoke mechanism, (b) idealized force acting on link 4.

The degree of freedom of the Scotch yoke mechanism is one. A single generalized coordinate is sufficient to define the equation of motion of it. The variables in this mechanism; θ in the position of link 2, x and y the position of link 3, and $x+a_4$ the position of link 4. $q=\theta$ are chosen for the generalized coordinate. Now the Lagrangian expression must be written as a function of θ and/or $\dot{\theta}$.

The sum of the kinetic energies of the moving links;

$$K=K_2+K_3+K_4=\frac{1}{2}I_{CG2}\dot{\theta}^2+\frac{1}{2}m_3\left(\dot{x}^2+\dot{y}^2\right)+\frac{1}{2}m_4\dot{x}^2 \tag{16}$$

A loop closure equation is in Equation (17).

$$\vec{AB}=\vec{AD}+\vec{DB} \tag{17}$$

The x-axis and y-axis components of this vector equation are written respectively.

$$x=a_2\cos\theta \quad \text{and} \quad y=a_2\sin\theta \tag{18}$$

The velocity equations can be found by taking the time derivatives of Equation (18).

$$\dot{x} = -a_2\dot{\theta}\sin\theta \quad \text{and} \quad \dot{y} = a_2\dot{\theta}\cos\theta \tag{19}$$

Equation (19) is substituted into Equation (16) and rearranged,

$$K = \frac{1}{2}\left(I_2 + m_3a_2^2 + m_4a_2^2\sin^2\theta\right)\dot{\theta}^2 \tag{20}$$

The x-axis can be taken as the reference axis for potential energy.

$$P = mgh = mgy = m_3ga_2\sin\theta \tag{21}$$

Lagrangian expression,

$$L = K - P = K = \frac{1}{2}\left(I_2 + m_3a_2^2 + m_4a_2^2\sin^2\theta\right)\dot{\theta}^2 - m_3ga_2\sin\theta \tag{22}$$

The partial derivative of Equation (22) concerning the generalized velocity for the first term of the Lagrange equation,

$$\left(\frac{\partial L}{\partial\dot{\theta}}\right) = \left(I_2 + m_3a_2^2 + m_4a_2^2\sin^2\theta\right)\dot{\theta} \tag{23}$$

and then its derivative concerning time.

$$\frac{d}{dt}\left(\frac{\partial L}{\partial\dot{\theta}}\right) = \left(I_2 + m_3a_2^2 + m_4a_2^2\sin^2\theta\right)\ddot{\theta} + 2m_4a_2^2\sin\theta\cos\theta\dot{\theta}^2 \tag{24}$$

The partial derivative of Equation (22) for the second term of the Lagrange equation concerning the generalized coordinate.

$$\frac{\partial L}{\partial\theta} = -m_3ga_2\cos\theta + m_4a_2^2\sin\theta\cos\theta\dot{\theta}^2 \tag{25}$$

The mathematical expression of the force F_{14} given in Figure 5(b) can be written as Equation (26).

$$F_{14} = \begin{Bmatrix} 0 & 0 \le \theta \le \pi \\ \dfrac{500(\theta-\pi)}{\pi} & \pi \le \theta \le 2\pi \end{Bmatrix} \tag{26}$$

Equation (14) can be specialized as follows for the effect of F_{14} acting on link 4 and τ acting on link 2 on the generalized axis.

$$Q_\theta = \vec{F}_{14}\cdot\frac{\partial\vec{r}_H}{\partial\theta} + \vec{\tau}\cdot\frac{\partial\vec{\theta}}{\partial\theta} \tag{27}$$

The elements of Equation (27) can be expressed in vectorial form as below,

$$\begin{aligned} &\vec{F}_{14} = -F_{14}\vec{i} \\ &\partial\vec{r}_H = x\vec{i} = \left(a_2\cos\theta + DC + CH\right)\vec{i} \\ &\vec{\tau} = \tau\,\vec{k} \\ &\partial\vec{\theta} = \theta\,\vec{k} \end{aligned} \tag{28}$$

The vectors in Equation (28) are substituted into Equation (27).

$$Q_\theta = \left(-F_{14}\vec{i}\right)\cdot\left(-a_2\sin\theta\,\vec{i}\right) + \left(\tau\,\vec{k}\right)\cdot\left(1\,\vec{k}\right) = F_{14}a_2\sin\theta + \tau \tag{29}$$

Equations (24, 25, 29) are substituted into Equation (13), and a dynamic equation is obtained. It is given in Equation (30).

$$\begin{aligned} &\left(I_2 + m_3a_2^2 + m_4a_2^2\sin^2\theta\right)\ddot{\theta} + \left(m_4a_2^2\sin\theta\cos\theta\right)\dot{\theta}^2 + \\ &m_3ga_2\cos\theta = F_{14}a_2\sin\theta + \tau \end{aligned} \tag{30}$$

It can be written more compactly;

$$J_{eqv}(\theta)\ddot{\theta} + C_{eqv}(\theta)\dot{\theta}^2 = Q_{eqv}(\theta,\dot{\theta},t) \tag{31}$$

where;

$$\begin{aligned} &J_{eqv}(\theta) = I_2 + m_3a_2^2 + m_4a_2^2\sin^2\theta \\ &C_{eqv}(\theta) = m_4a_2^2\sin\theta\cos\theta \\ &Q_{eqv}(\theta,\dot{\theta},t) = F_{14}a_2\sin\theta + \tau - m_3ga_2\cos\theta \end{aligned} \tag{32}$$

Here, J_{eqv} is the equivalent mass/mass moment of inertia reduced to the actuator (actuator, driver or motor) axis, C_{eqv} is the equivalent terms of Coriolis and/or centripetal, Q_{eqv} is the equivalent force/torque showing the spring, damping, actuator and external force/torque.

4. NUMERICAL SOLUTION OF EQUATION OF MOTION INCLUDING ACTUATION

Machine designers should observe the dynamic behaviour of the mechanisms before incorporating them into their designs. They must also ensure that the kinematics and kinetics of the mechanisms are in working order. Numerical simulation of equations of motion must be performed to obtain dynamic behaviours. Many numerical integration methods are used for the approximate solution of equations of motion. The fourth-order Runge Kutta method is used as an integration technique in this section. State-space approach is carried out for the solution.

The mechanism given in Figure 5 (a) is used in the packaging machine. Let us assume that 300 packages per minute are expected from this machine. Then it is expected to rotate at a speed of approximately 300 rpm. The graph of external force is given in Figure 5(b). A gear reducer and motor will be used to drive the mechanism at the desired speed, and let the moment of inertia of the reducer and the motor reduced to the crankshaft be I_{R+M} = 1.5 kg-m^2. The friction and damping forces are not taken

into account in the analysis. The equation of motion of the mechanism is given in Equation (31). The mass moment of inertia of the reducer and motor is added to J_{eqv} .

$$J_{eqv}(\theta) = I_2 + I_{R+M} + m_3 a_2^2 + m_4 a_2^2 \sin^2\theta \tag{33}$$

The synchronous speed of a 4-pole induction motor is 1500 rpm from Equation (1). However, 300 rpm is desired, so a gear reducer is necessary to reduce the speed by 1/5. It is possible to calculate the work done by the mechanism against only the force *F*. It can be found in the area under the force-displacement graph. In this case, since the linear displacement during the return from π to 2π will be twice the length of the 2nd link (stroke length = 2r), the work/energy in one revolution will be as follows,

$$Work = \frac{1}{2}(500)2r = \frac{1}{2}500*2*0.35 = 175\ Nm/rev \tag{34}$$

The average torque value in a cycle is:

$$Torque = M_{ave}*2\pi \Rightarrow M_{ave} = \frac{Work}{2\pi} = \frac{175}{2\pi} = 27.85\ Nm \tag{35}$$

The approximate average speed of the crank of the mechanism is as in Equation (36).

$$\omega_{ave} = Synchronous\ Speed * Reducer * \frac{1\,\text{min}}{60\ s} = 1500 * \frac{1}{5} * \frac{1}{60} = 5\frac{rev}{s} = 31.4\ \frac{rad}{s} \tag{36}$$

Then, the average power requirement to only the external force is as in Equation (37).

$$Power = Work * \omega_o = 175*5 = 875\ W \tag{37}$$

4.1. Approximate Determination of Speed Fluctuation Coefficient

Assuming that the crank will rotate at average speed ($\ddot{\theta} = 0$), Equation (31) is arranged as follows to find the reduced torque on the crankshaft:

$$\tau_{mot} = m_4 a_2^2 \sin\theta\cos\theta + m_3 g a_2 \cos\theta - F_{14} a_2 \sin\theta \tag{38}$$

The average moment value was previously found in Equation (35). It will be possible to approximately determine the energy fluctuation or speed fluctuation graphically. The graphical representation of these moments for a cycle is given in Figure 6.

Table 1. Allowed speed fluctuation coefficients in different systems.

System	*Allowed k_s*
Pumps, Cutting machines	1/5 – 1/30
Machine Tools, Textile Machinery	1/40 – 1/50
Generators	1/100 – 1/300
Automobiles	1/200 – 1/300
Aircraft engines	1/1000 – 1/2000

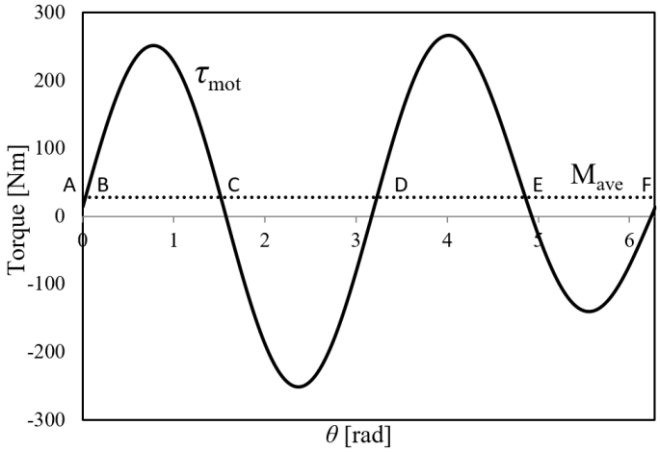

Fig. 6. Torque graph and average torque.

It is possible to easily calculate the energy levels at points *A*, *B*, *C*, *D*, *E* and *F*, where the motor torque intersects the average torque. These are given in Equations (39-43).

$$\begin{aligned} &Energy\ at\ A,\ E_A \\ &Energy\ at\ B, \\ &E_B = E_A + 0.2186 \end{aligned} \tag{39}$$

$$\begin{aligned} &Energy\ at\ C, \\ &E_C = E_B - 212.779 = E_A + 0.2186 - 212.779 = E_A - 212.56 \end{aligned} \tag{40}$$

$$\begin{aligned} &Energy\ at\ D, \\ &E_D = E_C + 301.8454 = E_A - 212.56 + 301.8454 = E_A + 89.2854 \end{aligned} \tag{41}$$

$$\begin{aligned} &Energy\ at\ E, \\ &E_E = E_D - 246.091 = E_A + 89.2854 - 246.091 = E_A - 156.8056 \end{aligned} \tag{42}$$

$$\begin{aligned} &Energy\ at\ F, \\ &E_F = E_E - 156.8056 = E_A \end{aligned} \tag{43}$$

While the energy level at point *C* is minimum, the energy level at *D* is maximum. Then the maximum energy fluctuation is:

$$\Delta E = (E_A + 89.2854) - (E_A - 212.56) = 301.8454\ Nm \tag{44}$$

We can determine the approximate speed fluctuation coefficient by using the reduced equivalent mass moment of inertia of the crankshaft given in Equation (33).

It $\sin^2\theta \approx 0$ is assumed,

$$k_s = \frac{\Delta E}{J_{eqv}\omega_{ave}^2} = \frac{\Delta E}{(I_2 + I_{R+M} + m_3 a_2^2)\omega_{ave}^2} = \frac{301.8454}{(0.02 + 1.5 + 4*0.35^2)*(10\pi)^2} = 0.155 \tag{45}$$

It is important to emphasize once again that the value found here is approximate. It can be said that this value is quite high even for a packaging machine. In this case, it is necessary to use a flywheel for the system. Table 1 shows different systems and allowed speed fluctuation coefficients [16].

4.2. Approximate Determination of Speed Fluctuation Coefficient with Numerical Solution

In this section, a numerical analysis including motor parameters is carried out. Let's choose a motor located in the seventh row of the motor catalogue given in Figure 3. The power of the selected motor is 2.2 kW, the nominal speed (N_n) is 1450 rpm, the nominal torque (M_n) is 14.5 Nm, the ratio of starting torque to nominal torque (M_{st} / M_n) is 2.8, and the ratio of breakdown torque to nominal torque (M_{bd} / M_n) is 3.6. While solving the differential equations, the time interval is chosen as 0.001 s. and the starting position and speed are chosen as zero. The dynamic behaviour of the system is given in Figure 7. Qbasic programming language has been used in the numerical simulations.

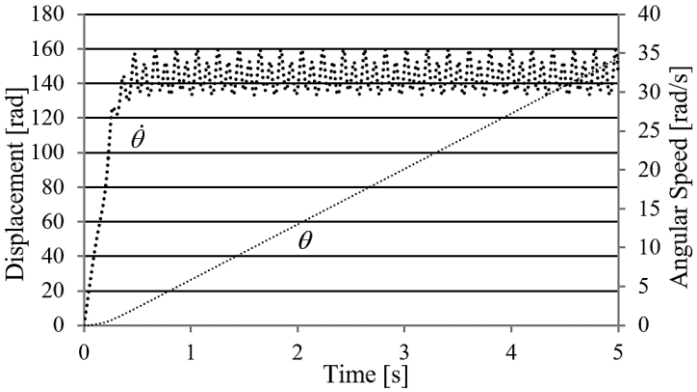

Fig. 7. Numerical solution of Scotch Yoke mechanism.

As shown in Figure 7, the result of the simulation shows that the crank speed range is $29.629\ rad/s < \dot{\theta} < 35.484\ rad/s$. In this case, the speed fluctuation coefficient is:

$$k_s = \frac{\omega_{\max} - \omega_{\min}}{\omega_{ave}} = \frac{35.484 - 29.629}{31.4} = 0.18647 \tag{46}$$

As mentioned above, this value is well above acceptable values. The time to reach the stable region is 0.354 s. If we assume that the speed fluctuation coefficient allowed for this system is $k_s = 1/50$, then the mass moment of inertia of the flywheel that should be used is approximately found as follows:

$$I_v = \frac{\Delta E}{k_s \omega_{ave}^2} = \frac{301.8454}{(0.02)*(10\pi)^2} = 15.3\ kgm^2 \tag{47}$$

Due to assumptions, it is better to select a bigger inertia value than found in Equation (47). The mass moment of inertia of the flywheel is added to the equivalent mass moment of inertia expression given in Equation (33). The numerical simulation is run with this modification, and the result is given in Figure 8.

As shown in Figure 8, the result of the simulation shows that the crank speed range is $30.665\ rad/s < \dot{\theta} < 31.452\ rad/s$. In this case, the speed fluctuation coefficient is:

$$k_s = \frac{\omega_{\max} - \omega_{\min}}{\omega_{ave}} = \frac{31.452 - 30.665}{31.4} = 0.02506 \tag{48}$$

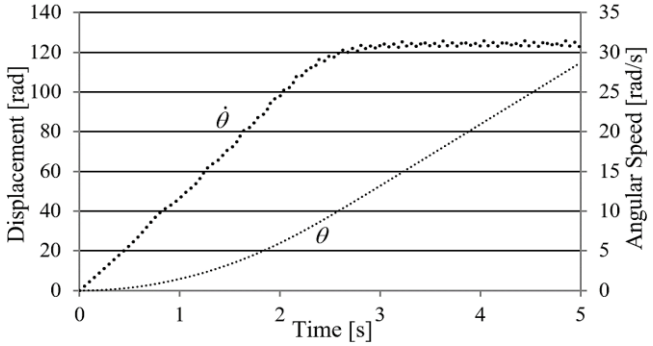

Fig. 8. Numerical solution of Scotch Yoke mechanism with flywheel.

The time to reach the stable region is approximately 3 seconds. It is understood that when adding a flywheel to the system, the desired speed fluctuation value is approached, but the time to reach the stable region increases.

If the time it takes for this motor to reach the stable region is not satisfactory and a lower value is desired, a more powerful/bigger motor should be selected. Let's choose the motor located in the ninth row of the motor catalogue given in Figure 3. The power of the selected motor is 4 kW, the nominal speed (N_n) is 1460 rpm, the nominal torque (M_n) is 26.2 Nm, the ratio of starting torque to nominal torque (M_{st} / M_n) is 2.8, and the ratio of breakdown torque to nominal torque (M_{bd} / M_n) is 3.8. When the motor data is entered as input to the model and the solution is re-done, the system behaviour is presented in Figure 9.

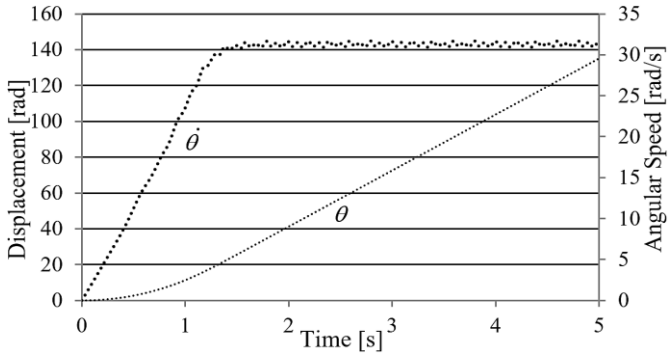

Fig. 9. Numerical solution of Scotch Yoke mechanism with flywheel and a bigger motor.

As shown in Figure 9, the result of the simulation shows that the crank speed range is $30.912\ rad/s < \dot{\theta} < 31.706\ rad/s$. In this case, the speed fluctuation coefficient is:

$$k_s = \frac{\omega_{\max} - \omega_{\min}}{\omega_{ave}} = \frac{31.706 - 30.912}{31.4} = 0.0253 \tag{49}$$

The time to reach the stable region is 1.5 seconds. While there is a significant improvement in time to reach the stable region, there is no significant change in the speed fluctuation coefficient.

In this study, smaller capacity motors shown in Figure 3 were also run in numerical simulations. However, the times for 1.1 kW and 1.5 kW capacity motors to reach the stable region were approximately 7 seconds and 4.5 seconds, respectively. It was also observed that they could not fully reach the average speed values. That is why a 2.2 kW motor was chosen first in the study.

5. CONCLUSIONS

In this study, analyses are presented on the selection of asynchronous AC motors that are frequently used in industry. If a precise analysis is required, it is necessary to know the torque values of the motor corresponding to all speeds. The authors can easily state that it is not very easy to access these graphics directly from motor catalogues. Kloss formulas, detailed in the study and obtained with different approaches, enable these graphs to be obtained.

As it is known, motors are the providers of movement that drive mechanisms and therefore machines. For this reason, a Scotch yoke mechanism, which is frequently used in industry, is given. The equation of motion of this mechanism was obtained by the Lagrange technique. A selected Kloss equation was included in the mathematical model prepared for numerical analysis. Therefore, the values in the motor catalogue can be entered into the model as input. The electromechanical system equation of motion which is a second-order ordinary differential equation includes the mechanism dynamic model and the Kloss equations containing the catalogue data of the selected motor. After that, some interpretations were made of the simulation results. By examining the speed values in the system response and calculating the speed fluctuation coefficient, it became necessary to add a flywheel to the system. In the simulation results obtained as a result of this addition, interpretations were made regarding the transition time to the stable region. If this period was desired to be shorter, a bigger motor from the same catalogue was preferred and the results were examined. As expected, it was observed that the selected bigger capacity motor reduced the time to reach the stable region, but did not cause a noticeable change in the value of the speed fluctuation coefficient.

This study was formed by the authors to address a deficiency seen in the literature. This study can be considered as a guide. Using motor catalogue values directly makes the study practical. In other words, it is a study in which both mechanical and driving systems come together and the steps to be followed are explained in order. If the design procedure can be applied properly as mentioned in the study, reliable results can be obtained through simulation studies before establishing an experimental setup. This guide can be easily adapted to any other application. What needs to be changed are the type of mechanism and the external force to be applied. It is thought that it will contribute to the studies of researchers interested in this subject.

References

[1] A. E. Fitzgerald, C. Kingsley Jr, S. D. Umans, *Electric Machinery*, Sixth Edition. New York, NY: McGraw-Hill, 2003.
[2] D. Gerling, *Electrical Machines Mathematical Fundamentals of Machine Topologies*. Berlin, Heidelberg; Springer, 2003.
[3] D. G. Alciatore, *Introduction to Mechatronics and Measurement Systems*, Fifth Edition. New York, NY: McGraw-Hill, 2019**.**
[4] NEMA Standards Publication No. MG 1-1998 Motors and Generators.
[5] E. Söylemez, *Dynamics of Machinery*, İstanbul: Birsen Press, 2007**.**
[6] J. J. Uicker, G. R. Pennock, J. E. Shigley, *Theory of Machines and Mechanisms*, Fifth Edition. New York, NY: Oxford University Press, 2017**.**
[7] J. Pedra, "On the determination of induction motor parameters from manufacturer data for electromagnetic transient program," *IEEE Transactions on Power Systems*, vol. 23, pp. 1709-1718, 2008.
[8] M. H. Haque, "Determination of NEMA design induction motor parameters from manufacturer data," *IEEE Transactıons on Energy Conversion*, 23(4), pp. 997-1004, 2008.
[9] N. Koljčević, Ž. Fuštić, M. Ćalasan, "Analytical solution for determination of induction machine acceleration based on Kloss equation," *Serbian Journal of Electrical Engineering*, 17(2), pp. 247-256, 2020.
[10] P. Aree, "Analytical approach to determine speed-torque curve of induction motor from manufacturer data," *Procedia Computer Science*, vol. 86, pp. 293-296, 2016.
[11] C. Kral, A. Haumer, H. Kapeller, V. Pascoli, "Modelling and simulation of a large chipper drive," *The Open Electrical & Electronic Engineering Journal*, vol. 3, pp. 21-28, 2009.
[12] J. Buksnaitis, "Analytical determination of mechanical characteristics of asynchronous motors by varying the electric current frequency," *Elektronika Ir Elektrotechnika*, 112(6), pp. 3-6, 2011.
[13] P. Aree, "Analytical determination of speed-torque and speed-current curves of single-cage induction motor under supply voltage and frequency variations," *The International Journal for Computation and Mathematics in Electrical and Electronic Engineering*, 37(6), pp. 2279-2298, 2018.
[14] ELK Motors, "IE3 Three phase motors, page 25," [Online]. Available: https://www.elkmotor.com.tr/tr/elk-motor-kataloglarimiz [Accessed: March 26, 2024].
[15] H. Baruh, *Analytical Dynamics*. Singapore; McGraw Hill, 1999.
[16] S. Singh, *Theory of machines: Kinematics and Dynamics*. Third Edition. India; Pearson, 2012.

Biographies

Mehmet Erkan Kütük received a Ph.D. degree from the Mechanical Engineering Department of Gaziantep University, Turkiye, in 2019. He works as an assistant professor at the Machine Theory and Dynamics Division of the Mechanical Engineering Department at Gaziantep University. The main research areas focus on mechanism analysis and synthesis, robotics, dynamics of machinery, and modelling and control of electromechanical systems.
E-mail: mekutuk@gantep.edu.tr

Sadettin Kapucu received a Ph.D. degree from the Mechanical Engineering Department of Gaziantep University, Türkiye, in 1994. He works as a professor at the Machine Theory and Dynamics Division of the Mechanical Engineering Department at Gaziantep University. His main research areas are on robotics, robot vision, vibration suppression, dynamics of machinery, industrial hydraulics, and mechatronics.
E-mail: kapucu@gantep.edu.tr